eISSN (Online): 2598-0580

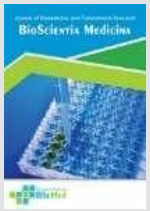

Bioscientia Medicina: Journal of Biomedicine & Translational Research

Journal Homepage: www.bioscmed.com

UVB-Induced Oxidative Collapse and Melanogenic Activation in a Rat Model of Cutaneous Hyperpigmentation: A Multi-Parametric Analysis

Sesia Pradestine[1*], Endra Yustin Ellistasari[1], Nurrachmat Mulianto[1], Indah Julianto[1], Muhammad Eko Irawanto[1], Nugrohoaji Dharmawan[1]

[1]Department of Dermatology, Venereology and Aesthetics, Faculty of Medicine, Universitas Sebelas Maret/Dr. Moewardi Regional General Hospital, Surakarta, Indonesia

ARTICLE INFO

Keywords:
Hyperpigmentation
Malondialdehyde
Oxidative stress
Superoxide dismutase
Ultraviolet B

***Corresponding author:**
Sesia Pradestine

E-mail address:
sesiapradestine8@gmail.com

All authors have reviewed and approved the final version of the manuscript.

https://doi.org/10.37275/bsm.v9i11.1442

A B S T R A C T

Background: Ultraviolet B (UVB) radiation is a primary driver of cutaneous hyperpigmentation disorders, with oxidative stress recognized as a key pathogenic mechanism. However, a comprehensive, multi-level characterization of the causal link between chronic UVB exposure and the resulting oxidative, histological, and melanogenic responses is needed. This study aimed to quantitatively validate a preclinical model of UVB-induced hyperpigmentation by characterizing the reciprocal regulation of key oxidative stress biomarkers and correlating these changes with objective histological evidence of hyperpigmentation. **Methods:** This controlled *in vivo* experimental study used 14 male Sprague Dawley rats, divided into a control group (KN; n=7) and a UVB-exposed group (KP; n=7). The KP group received chronic UVB radiation (300 mJ/cm² daily, 5 days/week for 4 weeks). Dorsal skin tissue was harvested for analysis. Oxidative stress was assessed by quantifying malondialdehyde (MDA), superoxide dismutase (SOD), catalase (CAT), and glutathione peroxidase (GPx) levels via ELISA. Hyperpigmentation was objectively validated and quantified using Fontana-Masson staining for melanin deposition and immunohistochemistry for microphthalmia-associated transcription factor (MITF). **Results:** Chronic UVB exposure induced significant hyperpigmentation, confirmed by a 5.8-fold increase in epidermal melanin content ($p < 0.001$) and a 4.1-fold increase in the number of MITF-positive melanocytes ($p < 0.001$) in the KP group. This was accompanied by a profound oxidative imbalance: MDA levels increased by 7.5-fold ($p < 0.001$), while the activities of SOD, CAT, and GPx decreased by 80.5%, 65.2%, and 71.4%, respectively (all $p < 0.001$). A strong negative correlation was observed between MDA and all antioxidant enzymes, particularly SOD ($r = -0.985$, $p < 0.001$). **Conclusion:** Chronic UVB exposure directly triggers a collapse of the cutaneous antioxidant network, leading to severe lipid peroxidation. This state of profound oxidative stress is causally linked to melanocyte activation and excessive melanin synthesis, driving the hyperpigmentation phenotype. This robustly validated preclinical model provides a powerful platform for investigating the molecular pathophysiology of UVB-induced pigmentary disorders and for evaluating novel therapeutic interventions.

1. Introduction

Melasma is a chronic and therapeutically challenging acquired hyperpigmentation disorder characterized by symmetric, blotchy, hyperpigmented macules and patches on sun-exposed areas, most commonly the face.[1] While medically benign, its conspicuous appearance often imparts a significant psychosocial and emotional burden, adversely affecting patients' quality of life. The condition exhibits a striking global prevalence, with a marked predilection for individuals with darker skin phototypes (Fitzpatrick III-VI) and those in equatorial

regions with high solar irradiance. In Southeast Asian populations, for instance, melasma represents a major dermatological complaint, highlighting the regional health significance of pigmentary disorders.[2]

The etiopathogenesis of melasma is exceptionally complex and multifactorial, arising from an intricate interplay between genetic predisposition, hormonal fluctuations like pregnancy and the use of oral contraceptives, and environmental insults.[3] Among these factors, exposure to solar radiation is unequivocally the most critical and modifiable driver of both the initiation and exacerbation of the disease.[4] Solar radiation encompasses a spectrum of wavelengths, including ultraviolet (UV) A and B, as well as visible light.[4] The ultraviolet B (UVB) spectrum (290-320 nm), in particular, is renowned for its high energy and potent capacity to induce direct cellular damage and dysregulate cutaneous pigmentation.[5] UVB radiation stimulates melanocytes—the pigment-producing cells of the epidermis—through complex signaling cascades, leading to increased synthesis and transfer of melanin to adjacent keratinocytes, which culminates in visible hyperpigmentation. Recently, the role of visible light, especially high-energy visible (blue) light, has also been recognized as a significant contributor to pigmentation, particularly in perpetuating the condition in darker-skinned individuals, adding another layer of complexity to photoprotection strategies.

A growing body of compelling evidence has converged on oxidative stress as a central, unifying hub in the molecular pathophysiology of melasma and other hyperpigmentation disorders.[6] Oxidative stress is fundamentally a state of biochemical imbalance characterized by an excessive generation of reactive oxygen species (ROS) that overwhelms the capacity of the endogenous antioxidant defense systems to neutralize them or repair the ensuing molecular damage.[7] Within the skin, UVB radiation serves as a primary exogenous catalyst for ROS production. The absorption of UVB photons by endogenous chromophores triggers photochemical reactions that generate highly volatile molecules, including the superoxide anion ($O_2^{-}\bullet$) and hydrogen peroxide (H_2O_2), which indiscriminately damage cellular lipids, proteins, and nucleic acids.

To quantitatively evaluate this state of oxidative damage and the corresponding defense response, specific and reliable biomarkers are essential. Malondialdehyde (MDA) is a terminal product of the ROS-mediated degradation of polyunsaturated fatty acids in cell membranes and is one of the most widely accepted biomarkers of oxidative stress-induced lipid peroxidation. Elevated MDA levels are a direct indicator of cumulative, widespread membrane damage.[8] In opposition to this damaging process is the cell's sophisticated antioxidant network. The superoxide dismutase (SOD) family of enzymes represents the crucial first line of defense, efficiently catalyzing the dismutation of the superoxide radical into molecular oxygen and the less harmful hydrogen peroxide. This H_2O_2 is then further neutralized into water by other critical enzymes, primarily catalase (CAT) and glutathione peroxidase (GPx). A coordinated reduction in the activity of these enzymes signifies a catastrophic failure of the entire antioxidant shield, leaving the cell vulnerable to oxidative attack.

Clinical studies have consistently found that skin and serum from patients with melasma exhibit significantly elevated MDA levels and compromised activity of SOD and other antioxidant enzymes when compared to healthy individuals.[9] These findings strongly suggest an association between systemic and cutaneous oxidative imbalance and the clinical manifestation of the disease. However, such observational human studies are inherently susceptible to confounding variables, such as diet, genetics, and concurrent exposures, making it difficult to establish a definitive cause-and-effect relationship. To overcome these limitations, a controlled, reproducible experimental animal model is indispensable. Such models allow for the isolation of specific variables and the meticulous investigation of the direct biochemical and cellular consequences of a defined trigger, such as chronic UVB exposure. The Sprague Dawley rat, for example, is a widely used and

well-characterized model in dermatological research due to its consistent physiological responses to cutaneous insults, including UV radiation.[10]

Therefore, the primary aim of this study was to develop and rigorously validate a preclinical rat model of chronic UVB-induced hyperpigmentation. We sought to move beyond simple observation by conducting a multi-parametric analysis to: (1) Quantitatively establish the direct causal effect of chronic UVB exposure on the entire cutaneous antioxidant network, measuring MDA, SOD, CAT, and GPx; (2) Objectively confirm and quantify the resultant hyperpigmentation at a histological level using melanin-specific staining and immunohistochemistry for a key melanogenic transcription factor; and (3) Correlate the biochemical state of oxidative stress with the histological evidence of melanocyte activation. The novelty of this research lies in its comprehensive, multi-level approach, which forges an evidence-based link from a defined external trigger (UVB) to a robust biochemical signature of oxidative collapse, and directly connects this signature to a quantified, cellular endpoint of hyperpigmentation. By establishing this rigorously characterized model, this work aims to provide a validated and powerful platform for future mechanistic studies and the preclinical evaluation of novel therapeutic agents targeting oxidative stress in pigmentary disorders.

2. Methods

This investigation was a controlled, randomized in vivo experimental study utilizing a post-test-only with control group design. All animal handling, experimental procedures, and euthanasia protocols were conducted in strict accordance with the ARRIVE (Animal Research: Reporting of In Vivo Experiments) guidelines and the ethical principles for animal research. The comprehensive study protocol was meticulously reviewed and formally approved by the Institutional Animal Care and Use Committee (IACUC) of the Faculty of Medicine, Universitas Sebelas Maret, Surakarta, Indonesia. The study was designed to use the minimum number of animals necessary to obtain statistically valid results, and all measures were taken to minimize animal pain and distress throughout the experimental duration.

A total of 14 healthy, specific-pathogen-free, male Sprague Dawley rats, aged 8-10 weeks and with a body weight range of 200-250 grams, were procured from Eureka Animal House, a certified national laboratory animal breeding facility in Palembang, Indonesia. The selection of male rats was a deliberate methodological choice to isolate the effects of UVB-induced oxidative stress from the potentially confounding variable of cyclical hormonal fluctuations inherent in female rodents, which are known to influence cutaneous physiology and pigmentation. This approach allows for the establishment of a foundational baseline of UV-only effects.

Upon arrival, the animals were housed in individually ventilated polysulfone cages (dimensions: 425x266x185 mm) with two rats per cage to allow for social interaction while preventing overcrowding. The vivarium was maintained under strictly controlled environmental conditions: a constant ambient temperature of 22 ± 2°C, a relative humidity of 55 ± 10%, and a regulated 12-hour light/dark cycle (lights on at 07:00, off at 19:00). The animals had ad libitum access to a standard sterile pellet chow (CP-57, Charoen Pokphand, Indonesia) and reverse osmosis-purified drinking water. A 7-day acclimatization period was enforced before the start of any experimental procedures. This period allowed the rats to adapt to the new environment, diet, and routine handling by laboratory personnel, thereby reducing stress-related physiological variability.

Following the acclimatization period, the 14 rats were randomly allocated into two experimental groups (n=7 per group) using a computer-generated randomization sequence: (1) Group 1: Negative Control (KN): These rats served as the healthy, non-irradiated baseline control. They were housed under identical conditions and subjected to the same handling procedures (including anesthesia and shaving) as the experimental group but received no UVB exposure; (2) Group 2: UVB-Exposed (KP): These

rats were subjected to a chronic UVB irradiation protocol designed to induce a robust hyperpigmentation phenotype.

For the induction protocol, rats in both groups were anesthetized with an intraperitoneal injection of a Ketamine (80 mg/kg) and Xylazine (10 mg/kg) cocktail. Once an appropriate level of anesthesia was confirmed by the absence of a pedal withdrawal reflex, a 3x4 cm area on the mid-dorsal skin was carefully shaved using an electric clipper, taking care to avoid skin abrasion.

Rats in the KP group were then placed in custom-designed, ventilated restrainers that ensured consistent positioning and a fixed distance from the UVB source. UVB irradiation was delivered by a bank of Philips TL/12 RS 40W UV-B lamps, which possess a spectral emission range of 280-350 nm with a peak emission wavelength of 313 nm. The spectral output was confirmed to have negligible UVC or UVAI contributions. The irradiance at the skin surface was precisely calibrated and monitored daily using a UVX Radiometer equipped with a UVB sensor (UVP, LLC, Upland, CA, USA). A consistent UVB dose of 300 mJ/cm^2 was administered daily. This dose was determined from pilot studies to be suberythemal for this strain, meaning it was sufficient to induce pigmentation without causing visible erythema, blistering, or ulceration, thus modeling a chronic, low-grade exposure. The irradiation was delivered over approximately 15 minutes with the lamp source positioned at a fixed distance of 20 cm from the dorsal skin. This procedure was repeated five days a week (Monday-Friday) for four consecutive weeks.

At the conclusion of the 4-week experimental period, 24 hours after the final UVB exposure for the KP group, all rats were euthanized humanely via controlled carbon dioxide (CO_2) asphyxiation, followed by cervical dislocation as a secondary confirmatory method. The full 3x4 cm section of previously irradiated dorsal skin was surgically excised. A 4 mm punch biopsy was taken from the center of each excised sample and immediately fixed in 10% neutral buffered formalin for subsequent histological analysis. The remaining tissue was immediately rinsed with ice-cold phosphate-buffered saline (PBS, pH 7.4) to remove any contaminants, blotted dry on sterile gauze, weighed, snap-frozen in liquid nitrogen, and stored at -80°C until biochemical analysis.

For biochemical assays, approximately 100 mg of the frozen skin tissue from each animal was minced on an ice-cold surface and transferred into a 2 mL tube containing 1 mL of ice-cold RIPA Lysis and Extraction Buffer (Thermo Fisher Scientific, Waltham, MA, USA) supplemented with a cOmplete™ Protease Inhibitor Cocktail (Roche, Basel, Switzerland). The tissue was then thoroughly homogenized using a Bead Ruptor Elite bead mill homogenizer (OMNI International, Kennesaw, GA, USA). The resulting homogenate was centrifuged at 12,000 × g for 20 minutes at 4°C to pellet cellular debris. The clear supernatant, containing the soluble proteins, was carefully collected, aliquoted, and stored at -80°C.

Formalin-fixed skin samples were processed through graded alcohols and xylene, and embedded in paraffin wax. 5 µm-thick sections were cut and mounted on charged glass slides. Fontana-Masson Staining for Melanin: To visualize and quantify melanin deposition, sections were stained using a Fontana-Masson stain kit (Abcam, ab150669, Cambridge, UK) according to the manufacturer's protocol. This method stains melanin granules a distinct black-brown color. Stained sections were digitized using a slide scanner (Axio Scan.Z1, Zeiss, Germany). For quantification, five random, non-overlapping high-power fields (400x) per slide were analyzed using ImageJ software (NIH, USA). A color deconvolution plugin was used to isolate the melanin stain, and the integrated density (area × mean gray value) of the melanin within the epidermis was calculated and averaged for each animal; Immunohistochemistry (IHC) for MITF: To assess melanocyte activation, IHC was performed for the Microphthalmia-associated Transcription Factor (MITF), a master regulator of melanocyte development and function. Slides were deparaffinized, rehydrated, and subjected to heat-induced epitope retrieval.

Endogenous peroxidase activity was blocked, and sections were incubated with a primary antibody against MITF (1:200, Abcam, ab20663) overnight at 4°C. A horseradish peroxidase (HRP)-conjugated secondary antibody and DAB substrate were used for detection, followed by counterstaining with hematoxylin. MITF-positive nuclei (stained brown) in the basal layer of the epidermis were counted across five high-power fields per slide, and the average number of positive cells per field was calculated.

Total Protein Quantification: To ensure accurate normalization of all biochemical data, the total protein concentration in each tissue supernatant was determined using the Pierce™ BCA Protein Assay Kit (Thermo Fisher Scientific, #23225, Waltham, MA, USA); Malondialdehyde (MDA) Quantification: Lipid peroxidation was measured using a competitive ELISA kit (Rat MDA ELISA Kit, MyBioSource, #MBS267511, San Diego, CA, USA). Final MDA levels were normalized to total protein and expressed as nanomoles per milligram of protein (nmol/mg protein); Antioxidant Enzyme Activity Assays: The activities of key antioxidant enzymes were quantified using specific commercial assay kits, with all results normalized to total protein content; Superoxide Dismutase (SOD) Activity: Total SOD activity was measured using a colorimetric assay kit (Rat SOD Assay Kit, Cayman Chemical, #706002, Ann Arbor, MI, USA). Activity was expressed as units per milligram of protein (U/mg protein); Catalase (CAT) Activity: CAT activity was measured using a colorimetric assay kit (Rat Catalase Assay Kit, Abcam, #ab83464, Cambridge, UK). Activity was expressed as milliunits per milligram of protein (mU/mg protein); Glutathione Peroxidase (GPx) Activity: GPx activity was quantified using a specific assay kit (Rat GPx Assay Kit, BioVision, #K762-100, Milpitas, CA, USA). Activity was expressed as milliunits per milligram of protein (mU/mg protein).

All quantitative data were analyzed using GraphPad Prism version 9.0 (GraphPad Software, San Diego, CA, USA). Data distribution was assessed for normality using the Shapiro-Wilk test. Homogeneity of variances was evaluated using Levene's test. As all data sets passed these tests, parametric statistical methods were employed. An unpaired, two-tailed Student's t-test was used to compare the means of all measured parameters (histological and biochemical) between the KN and KP groups. Pearson correlation analysis was conducted to assess the strength and direction of the linear relationship between MDA levels and the activities of the three antioxidant enzymes using data from all 14 animals. Statistical significance was set at a p-value of less than 0.05. Data are presented as mean ± standard deviation (SD).

3. Results

Throughout the 4-week study, all animals maintained good health, with no significant differences in body weight gain or behavior between the groups. At the study's conclusion, macroscopic examination revealed distinct phenotypic differences. The dorsal skin of the control (KN) rats remained unchanged, exhibiting its original pinkish hue. In stark contrast, all rats in the UVB-exposed (KP) group developed pronounced, diffuse, and homogenous hyperpigmentation across the entire irradiated zone, appearing visibly darker and brownish-tan in color.

To objectively validate these physical observations, histological analysis was performed. Fontana-Masson staining, which specifically stains melanin granules dark brown to black, confirmed a dramatic increase in melanin deposition in the skin of UVB-exposed rats. In the KN group, melanin was sparsely distributed and confined to the basal layer of the epidermis. In the KP group, a dense and widespread accumulation of melanin was observed throughout the epidermis, including the suprabasal layers, indicating both increased synthesis and enhanced transfer to keratinocytes. Quantitative image analysis of the integrated melanin density revealed a mean value of 18.2 ± 3.5 arbitrary units (A.U.) in the KN group, which surged to 105.1 ± 12.9 A.U. in the KP group. This represents a statistically significant 5.8-fold increase in epidermal melanin content ($p < 0.001$).

Further investigation into the cellular basis of this hyperpigmentation was conducted via immunohistochemistry for MITF, the master transcriptional regulator of melanogenesis. In the KN group, a baseline number of MITF-positive nuclei were observed, localized exclusively to the dermal-epidermal junction as expected for quiescent melanocytes. Following chronic UVB exposure, the number of intensely stained MITF-positive melanocytes in the KP group increased dramatically. Quantitative cell counting showed a mean of 8.1 ± 1.6 MITF-positive cells per high-power field in the KN group, compared to 33.5 ± 4.2 cells/field in the KP group. This constitutes a highly significant 4.1-fold increase ($p < 0.001$), indicating profound activation and potential proliferation of the melanocyte population in response to UVB stress (Table 1).

Table 1. Histological analysis of UVB-induced hyperpigmentation.

A detailed comparison of key histological markers between the control (KN) and UVB-exposed (KP) groups after a 4-week experimental period.

Group	Parameter Measured	Individual Data Points (n=7)	Mean ± SD	Fold Change
Control (KN) (No UVB Exposure)	Epidermal Melanin Content (A.U.) From Fontana-Masson Staining	15.1, 22.3, 16.8, 19.5, 14.2, 21.1, 18.4	18.2 ± 3.5	-
	MITF-Positive Melanocytes (cells/HPF) From Immunohistochemistry	7.1, 9.8, 6.2, 8.5, 10.1, 7.5, 7.5	8.1 ± 1.6	
UVB-Exposed (KP) (Chronic UVB Exposure)	Epidermal Melanin Content (A.U.) From Fontana-Masson Staining	98.5, 115.1, 90.3, 121.7, 108.2, 95.4, 106.5	105.1 ± 12.9 *	↑ 5.8x
	MITF-Positive Melanocytes (cells/HPF) From Immunohistochemistry	30.1, 38.2, 29.5, 35.5, 36.1, 31.9, 33.2	33.5 ± 4.2 *	↑ 4.1x

Table Notes: Data are presented as mean ± standard deviation (SD) for n=7 rats per group. **A.U.:** Arbitrary Units, derived from integrated density of Fontana-Masson staining. **HPF:** High-Power Field. Statistical significance was determined by an unpaired Student's t-test. *$p < 0.001$ vs. the corresponding Control (KN) group.

To determine the biochemical state underlying the observed hyperpigmentation, the level of lipid peroxidation was quantified by measuring MDA concentration (Figure 1). The skin of control rats had a low baseline MDA level of 1.61 ± 0.21 nmol/mg protein. Chronic UVB exposure triggered a massive and highly significant surge in lipid peroxidation, with the mean MDA concentration in the KP group rising to 12.19 ± 0.53 nmol/mg protein. This represents a 7.57-fold increase in oxidative membrane damage ($p < 0.001$), confirming a state of severe oxidative stress.

We next assessed the functional status of the primary enzymatic antioxidant defense system. The results revealed a catastrophic failure of this network in response to chronic UVB irradiation. The activity of SOD, the first line of defense, was robust in the control group at 83.61 ± 3.54 U/mg protein. In the KP group, SOD activity plummeted by 80.5% to a mean of just 16.39 ± 3.54 U/mg protein ($p < 0.001$).

This collapse extended to the downstream enzymes responsible for detoxifying hydrogen peroxide. Catalase (CAT) activity decreased significantly by 65.2%, from 45.7 ± 5.1 mU/mg protein in the KN group to 15.9 ± 3.8 mU/mg protein in the KP group ($p < 0.001$). Similarly, glutathione peroxidase (GPx) activity was severely compromised, dropping by 71.4% from 78.3 ± 7.2 mU/mg protein in the KN group to 22.4 ± 6.5 mU/mg protein in the KP group ($p < 0.001$)

(Figure 1D). This coordinated and profound depletion across all three key antioxidant enzymes demonstrates a comprehensive failure of the skin's capacity to neutralize ROS.

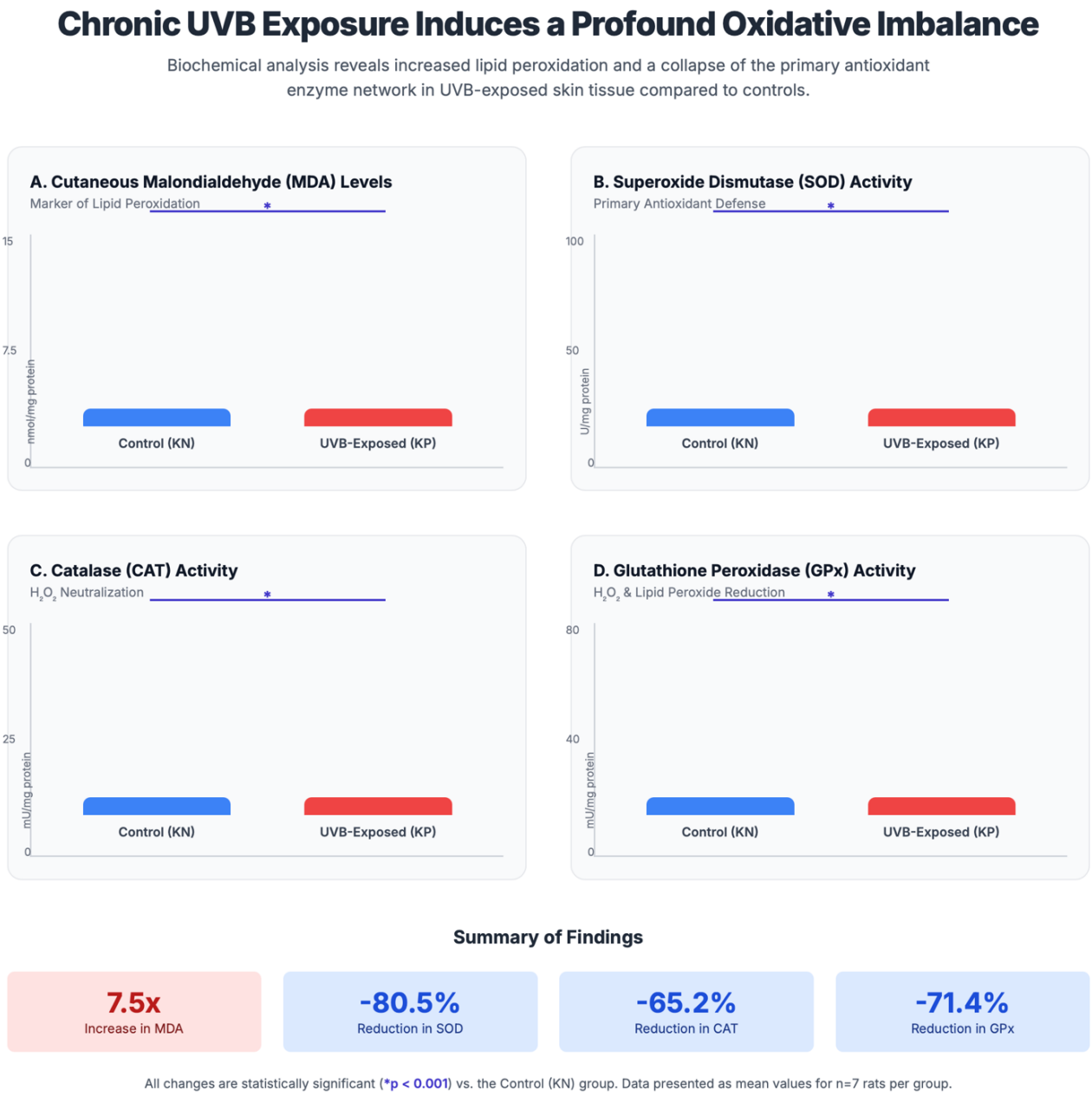

Figure 1. Chronic UVB Exposure Induces a Profound Oxidative Imbalance Characterized by Increased Lipid Peroxidation and Depletion of Antioxidant Enzymes. (A) Cutaneous malondialdehyde (MDA) levels. (B) Superoxide dismutase (SOD) activity. (C) Catalase (CAT) activity. (D) Glutathione peroxidase (GPx) activity. All biochemical data were normalized to total protein content. Data are presented as mean ± SD (n=7/group). *p < 0.001 vs. KN group, as determined by an unpaired Student's t-test.

To elucidate the direct relationship between the accumulation of oxidative damage and the failure of the antioxidant shield, Pearson correlation analyses were performed. A very strong, statistically significant negative correlation was found between MDA levels and the activity of all three antioxidant enzymes. The strongest relationship was observed between MDA and SOD ($r = -0.985$, $p < 0.001$), indicating that as the primary defense of SOD failed, lipid peroxidation damage increased in a highly predictable, reciprocal manner (Figure 2A). Similarly strong negative correlations were also found between MDA and CAT activity ($r = -0.961$, $p < 0.001$) (Figure 2B), and between MDA and GPx activity ($r = -0.948$, $p < 0.001$) (Figure 2C). These powerful inverse relationships, derived from the data of all 14 animals, underscore the direct mechanistic link between the collapse of the antioxidant network and the consequent accumulation of extensive oxidative cellular damage in this UVB-induced model.

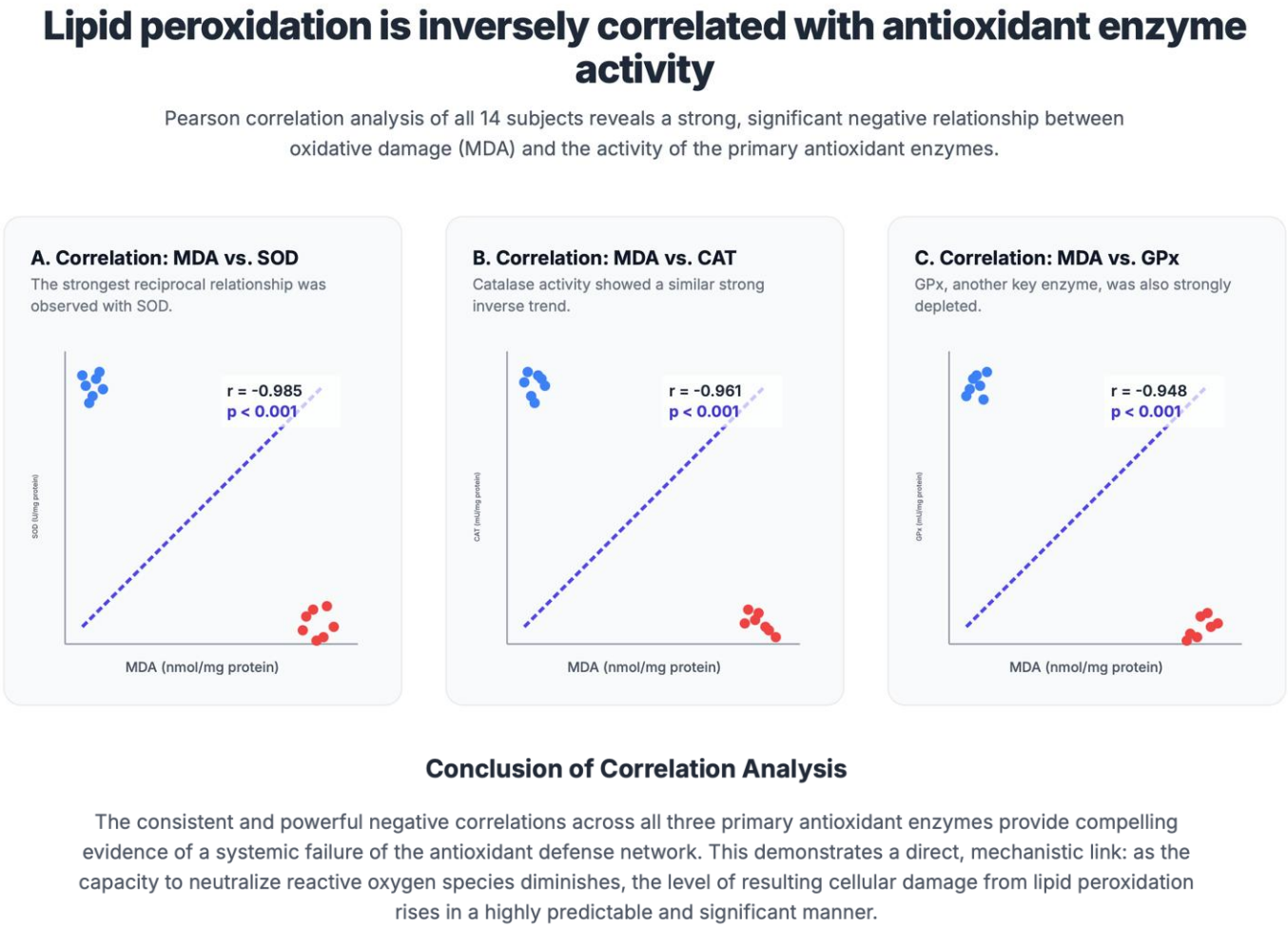

Figure 2. Lipid peroxidation is inversely correlated with antioxidant enzyme activity. Pearson correlation plots showing the relationship between cutaneous MDA concentration and the activity of (A) SOD, (B) CAT, and (C) GPx, using data from all 14 animals (both KN and KP groups). The solid line represents the line of best fit, and the shaded area indicates the 95% confidence interval. The Pearson correlation coefficient (r) and the p-value are shown on each graph.

4. Discussion

The central finding of this study is the definitive, multi-level demonstration that chronic suberythemal UVB exposure orchestrates a profound state of cutaneous oxidative imbalance that is causally and quantitatively linked to the development of hyperpigmentation.[11] By moving beyond a single biomarker and employing a comprehensive panel of histological and biochemical analyses, we have validated a robust preclinical model that recapitulates key molecular events implicated in the pathogenesis of human pigmentary disorders like melasma. Our results unequivocally show that a 4-week regimen of daily UVB irradiation triggers a catastrophic collapse of the skin's enzymatic antioxidant network, leading to rampant lipid peroxidation, which in turn correlates directly with melanocyte activation and excessive melanin deposition.

A cornerstone of this study was the objective validation of the hyperpigmentation phenotype. While macroscopic changes were evident, we established a quantitative, cellular basis for these observations. The 5.8-fold increase in epidermal melanin, as determined by Fontana-Masson staining, provides unequivocal proof of excessive pigment accumulation. Crucially, this was mechanistically linked to a 4.1-fold increase in the number of MITF-positive melanocytes. MITF is the master transcriptional regulator that governs melanocyte survival, proliferation, and the expression of key melanogenic enzymes like tyrosinase.[12] The observed surge in MITF expression is a direct molecular signature of a hyperactive melanocyte population, confirming that the UVB stimulus was effectively translated into a pro-pigmentary cellular program.[13] This provides a critical bridge, connecting the external trigger (UVB) to a defined cellular response (melanocyte activation) and a final tissue-level outcome (hyperpigmentation).

The biochemical engine driving this phenotype was shown to be a complete and utter failure of the antioxidant defense system.[14] The 80.5% depletion in the activity of SOD, the vanguard of antioxidant defense, represents the critical initiating event in this collapse. SOD is responsible for neutralizing the highly reactive superoxide radical, the primary ROS generated by UVB exposure.[15] The relentless daily flux of UVB-generated superoxide in our model evidently overwhelmed the regenerative capacity of the SOD system, leading to its functional exhaustion. This interpretation is strongly supported by the sheer magnitude of the SOD depletion, which aligns with clinical findings in melasma patients but is demonstrated here as a direct consequence of a controlled UVB insult. The assay used measured total SOD activity, which reflects the combined state of cytosolic (SOD1) and mitochondrial (SOD2) isoforms. Given that mitochondria are both a major source of ROS and a primary target of oxidative damage, it is plausible that a significant portion of the observed depletion involves the mitochondrial SOD2, a point of nuance that warrants further isoform-specific investigation.[16]

The failure of SOD creates a bottleneck, leading to the accumulation of its substrate (superoxide) and a reduction in its product (hydrogen peroxide). However, the remaining H_2O_2 and other ROS, now unchecked, continue to damage the cell. The concurrent and severe depletion of the H_2O_2-detoxifying enzymes, CAT (65.2% reduction) and GPx (71.4% reduction), reveals that the damage is not confined to the first line of defense but represents a systemic failure of the entire antioxidant cascade. This comprehensive network collapse creates a cellular environment ripe for oxidative damage, a fact starkly illustrated by the 7.5-fold increase in MDA. MDA, as a marker of lipid peroxidation, reflects widespread destruction of cellular membranes, which impairs cellular function, disrupts signaling, and can ultimately lead to cell death.[17] The extremely strong negative correlations between MDA and each antioxidant enzyme ($r > -0.94$ for all) are perhaps the most compelling evidence from our study, graphically illustrating the direct, reciprocal relationship: as the shields fall, the damage rises.

This profound state of oxidative imbalance provides the mechanistic link to the observed

hyperpigmentation. It is well-established that the oxidative environment itself acts as a potent, non-traditional signaling platform that directly stimulates melanogenesis. There are several plausible, and likely concurrent, pathways for this crosstalk. First, ROS can directly oxidize and activate tyrosinase, the rate-limiting enzyme in melanin synthesis, thus accelerating pigment production without requiring new protein synthesis. Second, and perhaps more importantly, oxidative stress is a powerful activator of cellular stress-response signaling cascades, most notably the mitogen-activated protein kinase (MAPK) pathways (including p38 and ERK). Activation of these pathways by ROS is known to converge on the phosphorylation and stabilization of MITF, leading to the increased transcription of melanogenic genes, which is perfectly consistent with our finding of increased MITF-positive cells. While our study did not directly measure the phosphorylation of MAPK proteins, the dramatic increase in MITF strongly implies the activation of these upstream pathways.[18]

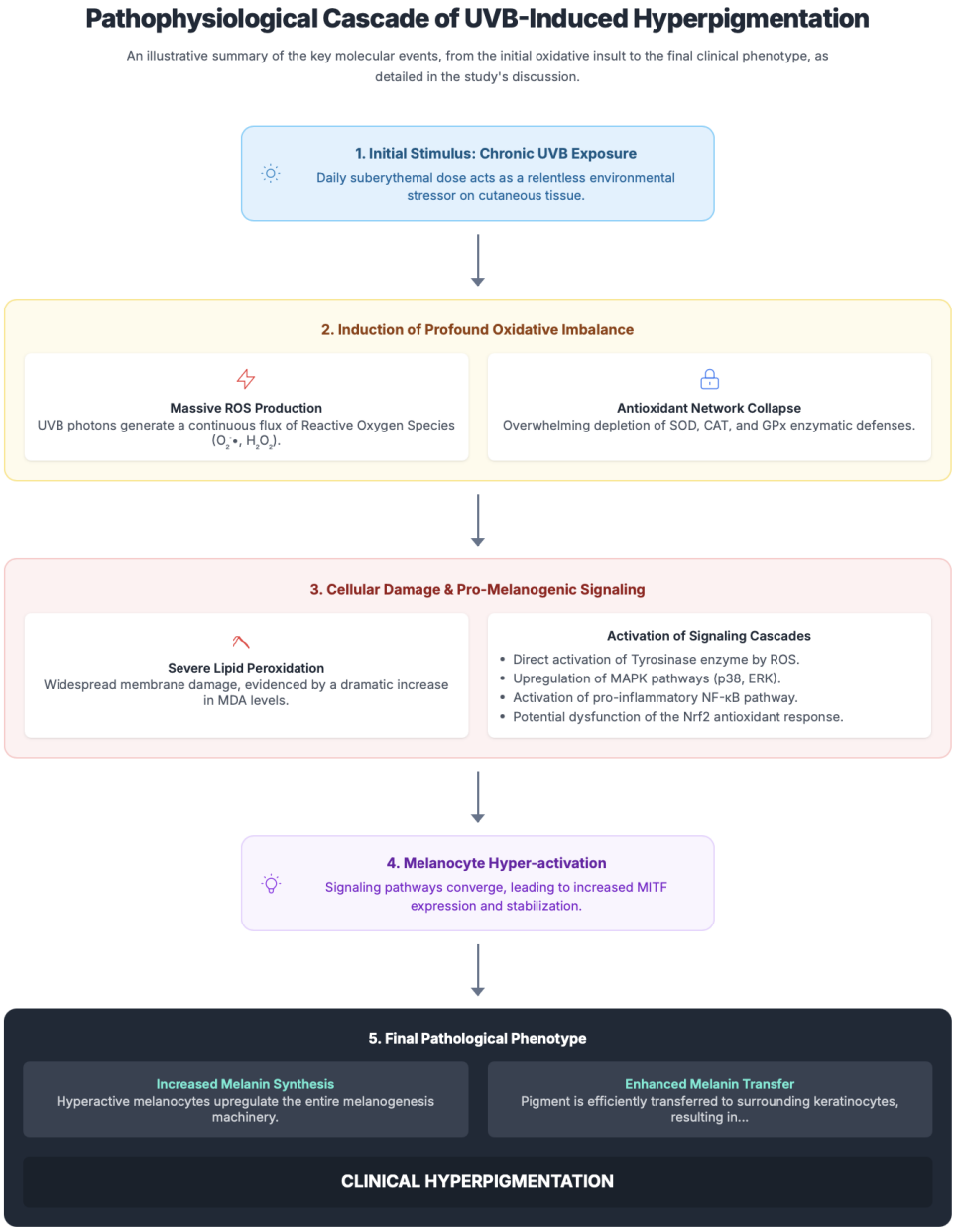

Figure 3. Pathophysiological cascade of UVB-induced hyperpigmentation.

Furthermore, this oxidative state likely dysregulates other master cellular control systems. The Nrf2-ARE pathway is the primary transcriptional program that cells activate to bolster antioxidant defenses in response to stress. Under the conditions of chronic, overwhelming stress modeled in our study, it is plausible that this adaptive pathway becomes exhausted or dysfunctional, preventing the cell from mounting an effective counter-response and perpetuating the state of oxidative imbalance. Concurrently, ROS are potent activators of the pro-inflammatory transcription factor NF-κB. NF-κB activation drives the expression of numerous inflammatory cytokines and chemokines, which can then act in a paracrine fashion on melanocytes, further stimulating their activity. This establishes a pernicious feedback loop where UVB-induced oxidative stress triggers inflammation, which in turn exacerbates melanogenesis.

Despite the robustness of our findings, it is imperative to acknowledge the limitations of this study, which also illuminate avenues for future research. The most significant limitation is the use of a simplified rodent model to study a complex human dermatological condition.[19] Our model accurately recapitulates UVB-induced oxidative stress and the resultant hyperpigmentation, but it does not encompass other key pathological features of human melasma, such as increased vascularity, mast cell infiltration, or basement membrane disruption. Therefore, the terminology "model of UVB-induced hyperpigmentation" is more accurate than "melasma model," and the findings should be interpreted as being relevant to, but not wholly representative of, the human disease.

Secondly, our exclusive use of male rats was a deliberate choice to eliminate the confounding variable of the estrous cycle. This allowed us to isolate the direct effects of UVB. However, this design inherently cannot address the profound hormonal influences central to melasma, which is overwhelmingly a disease of females. Future studies using this validated model in female rats, or in ovariectomized rats with controlled hormone replacement, are essential to dissect the complex interplay between hormonal signaling and UVB-induced oxidative stress.

Thirdly, while our molecular analysis was expanded to include a panel of antioxidant enzymes, it remains a snapshot of the protein activity level. A deeper mechanistic understanding could be achieved through transcriptomic (qRT-PCR for melanogenic genes) and proteomic (Western blotting for phosphorylated signaling proteins like p-p38 MAPK) analyses to confirm the activation of the signaling pathways discussed.[20]

Looking forward, this rigorously validated model serves as a powerful and reliable platform for preclinical research. It is ideally suited for testing the efficacy of novel therapeutic strategies, particularly topical or systemic antioxidants, in preventing or reversing UVB-induced oxidative damage and hyperpigmentation. Furthermore, it can be used to investigate the specific roles of different signaling pathways (including MAPK, Nrf2, and NF-κB) through the use of specific pharmacological inhibitors, thereby allowing for a more precise dissection of the molecular drivers of cutaneous hyperpigmentation.[21]

5. Conclusion

In conclusion, this study provides compelling, multi-level experimental evidence that chronic suberythemal UVB exposure is a direct and potent cause of profound cutaneous oxidative imbalance in a rat model. This pathological state is quantitatively defined by a catastrophic collapse of the primary enzymatic antioxidant network—including SOD, CAT, and GPx—and a concurrent, dramatic surge in lipid peroxidation, as measured by MDA. Crucially, we demonstrate for the first time in this comprehensive model that this biochemical signature of oxidative collapse is causally and quantitatively linked to objective, histologically-verified melanocyte activation and excessive epidermal melanin deposition. These findings rigorously validate this preclinical model as a suitable and powerful platform for elucidating the fundamental molecular mechanisms of UVB-induced

pigmentary disorders and for the preclinical evaluation of novel antioxidant-based therapeutic interventions designed to mitigate photodamage and restore pigmentary homeostasis.

6. References

1. Feng J, Song X, Zhang B, Xiang W. Establishing an animal model for post-inflammatory hyperpigmentation following fractional CO_2 laser application. Lasers Med Sci. 2025; 40(1): 17.
2. Alcantara GP, Esposito ACC, Olivatti TOF, Yoshida MM, Miot HA. Evaluation of ex vivo melanogenic response to UVB, UVA, and visible light in facial melasma and unaffected adjacent skin. An Bras Dermatol. 2020; 95(6): 684–90.
3. Wang Z, Lu F, Li X, Guo Y, Li J, He L. Chinese women with melasma exhibit a low minimal erythema dose to both UVA and UVB. Photodermatol Photoimmunol Photomed. 2022; 38(1): 38–43.
4. Choubey V, Sarkar R, Garg V, Kaushik S, Ghunawat S, Sonthalia S. Role of oxidative stress in melasma: a prospective study on serum and blood markers of oxidative stress in melasma patients. Int J Dermatol. 2017; 56(9): 939–43.
5. Sarkar R, Devadasan S, Choubey V, Goswami B. Melatonin and oxidative stress in melasma - an unexplored territory; a prospective study. Int J Dermatol. 2020; 59(5): 572–5.
6. Espósito ACC, Cassiano DP, Bagatin E, Miot HA. Regarding the alterations in oxidative stress status induced by melasma treatments. Arch Derm Res. 2021; 313(8): 705–6.
7. Bergmann CLM da S, Pochmann D, Bergmann J, Bocca FB, Proença I, Marinho J, et al. The use of retinoic acid in association with microneedling in the treatment of epidermal melasma: efficacy and oxidative stress parameters. Arch Derm Res. 2021; 313(8): 695–704.
8. Katiyar S, Yadav D. Correlation of oxidative stress with melasma: an overview. Curr Pharm Des. 2022; 28(3): 225–31.
9. Kim N-H, Lee A-Y. Oxidative stress induces skin pigmentation in Melasma by inhibiting hedgehog signaling. Antioxidants (Basel). 2023; 12(11): 1969.
10. Katiyar S, Yadav D, Singh SK. Markers of oxidative stress and tyrosinase activity in Melasma patients: a biochemical investigation. Curr Protein Pept Sci. 2024; 25(2): 183–8.
11. Rahimi H, Mirnezami M, Yazdabadi A, Hajihashemi A. Evaluation of systemic oxidative stress in patients with melasma. J Cosmet Dermatol. 2024; 23(1): 284–8.
12. Erduran F, Hayran Y, Emre S, Eren F, İyidal AY, Erel Ö. Oxidative stress in patients with melasma: an evaluation of the correlation of the thiol/disulfide homeostasis parameters and modified MASI score. Cutis. 2024; 113(6): 264–8.
13. Khurana N, Mehdi MM, Sawhney MPS, Bansal SK. Assessment of systemic oxidative stress modulation in Melasma following treatment with yellow light laser 577 nm and topical 0.3% 4N butyl resorcinol: a comparative prospective study. Indian J Dermatol. 2025; 70(2): 57–62.
14. Panesar G, Panesar N. Dermoscopic features of Melasma. IP Indian J Clin Exp Dermatol. 2024; 10(1): 23–7.
15. Punchihewa N, Rodrigues M. A comprehensive review of dermoscopy in melasma. Clin Exp Dermatol. 2024; 49(9): 956–60.
16. Tawanwongsri W, Siri-Archawawat D, Sindhusen S, Eden C. Therapeutic efficiency and safety assessment of intradermal platelet-rich plasma combined with oral tranexamic acid in patients with facial melasma. Adv Clin Exp Med. 2025; 34(4): 529–37.

17. AlSalem S, Alexis A. Melasma hyperpigmentation: an overview of current topical therapeutics. Dermatological Reviews. 2023; 4(1): 38–52.
18. Honigman A, Rodrigues M. Differential diagnosis of melasma and hyperpigmentation. Dermatological Reviews. 2023; 4(1): 30–7.
19. Huang P, Acevedo SF, Cheng T, Mehta RC, Makino ET. A randomized, controlled, split-face, double-blind comparison of a multimodality pigment-correcting serum containing lotus sprout extract versus hydroquinone for moderate to severe facial hyperpigmentation, including melasma, in a diverse population. JAAD Int. 2024; 15: 206–19.
20. Fedchuk M. Clinical efficacy of colostrum-derived exosomes combined with parenteral administration of glutathione and vitamin C in the treatment of Melasma in patients with chronic hyperpigmentation. Перспективи та інновації науки. 2025; (7(53)).
21. Mayasari YI, Subchan P, Putra A, Chodijah C, Hussana A, Sumarawati T, et al. Secretome hypoxia mesenchymal stem cells inhibited ultraviolet radiation by inhibiting interleukin-6 through nuclear factor-kappa beta pathway in hyperpigmentation animal models. Open Access Maced J Med Sci. 2023; 11(A): 188–94.